Experimental Neurology 229 (2011) 120–131

Contents lists available at ScienceDirect

Experimental Neurology

journal homepage: www.elsevier.com/locate/yexnr

Nasal OEC transplantation promotes respiratory recovery in a subchronic rat model of cervical spinal cord contusion

J.C. Stamegna [a,b,1], M.S Felix [a,b,1], J. Roux-Peyronnet [a,b], V. Rossi [a,b], F. Féron [c,d], P. Gauthier [a,b], V. Matarazzo [a,b,*]

[a] Centre de Recherche en Neurobiologie et Neurophysiologie de Marseille, CRN2M, CNRS UMR6231, 13397 Marseille, France
[b] Université Paul Cézanne, 13397 Marseille, France
[c] Neurobiologie des Interactions Cellulaires et Neurophysiopathologie, NICN, CNRS UMR 6184, Université de la Méditerranée, 13344 Marseille, France
[d] Centre d'Investigations Cliniques en Biothérapie CIC-B 510, AP-HM, Institut Paoli Calmettes, Inserm, Université de la Méditerranée, Marseille, France

ARTICLE INFO

Article history:
Received 28 April 2010
Revised 2 July 2010
Accepted 7 July 2010
Available online 12 July 2010

Keywords:
OEC
Breathing
Cervical contusion
Phrenic
Diaphragm
Recovery

ABSTRACT

Engraftment of nasal olfactory ensheathing cells (OEC) is considered as a promising therapeutic strategy for spinal cord repair and one clinical trial has already been initiated. However, while the vast majority of fundamental studies were focused on the recovery of locomotor function, the efficiency of this cellular tool for repairing respiratory motor dysfunction, which affects more than half of paraplegic/tetraplegic patients, remains unknown. Using a rat model that mimics the mechanisms encountered after a cervical contusion that induces a persistent hemi-diaphragmatic paralysis, we assessed the therapeutic efficiency of a delayed transplantation (2 weeks post-contusion) of nasal OECs within the injured spinal cord. Functional recovery was quantified with respiratory behavior tests, diaphragmatic electromyography and neuro-electrophysiological recording of the phrenic motoneurons while axogenesis was evaluated using immunohistochemistry. We show that 3 months post-transplantation, nasal OECs improve i) breathing movements, ii) activities of the ipsilateral diaphragm and corresponding phrenic nerve, and iii) axonal sprouting in the injury site. We also demonstrate that this functional partial recovery is mediated by the restoration of ipsilateral supraspinal command. Our study brings further evidence that olfactory ensheathing cells could have clinical application especially in tetraplegic patients with impaired breathing movements. This article is part of a Special Issue entitled: Understanding olfactory ensheathing glia and their prospect for nervous system repair.

Introduction

Spinal cord injury (SCI) is one of the leading causes of disabilities in young adults. An impaired transmission in sensory-motor neurons, including autonomic neurons, induces functional deficits and compromises life expectancy. Cervical injuries, which account for half of SCI cases (Jackson et al., 2004), are the most debilitating because they generally sever the bulbo-spinal respiratory drive to phrenic motoneuron pools (C3–C5) and, as a consequence, generate a diaphragm dysfunction. Mostly, cervically injured individuals require intensive post-SCI care with chronic respiratory ventilation assistance (Berlly and Shem, 2007). Respiratory symptoms include reduced vital capacity and secondary complications such as pulmonary infections (Berlly and Shem, 2007; Brown et al., 2006). It is therefore of prime importance to develop strategies aiming to restore respiratory capacities.

Although effective treatments for SCI are limited, most recently rehabilitative strategies such as cellular and molecular therapies have been tested in animal models and some clinical trials have been initiated. Implantation of olfactory ensheathing cells (OECs) seems to be one of the most promising (Kocsis et al., 2009; Raisman and Li, 2007). While the majority of the transplantation studies have used olfactory bulb-derived OECs (central), OECs can be also prepared from the lamina propria of the olfactory mucosa (peripheral) by nasal biopsy (Bianco et al., 2004; Richter and Roskams, 2008). The olfactory mucosa cells have already been autologously transplanted in paraplegic patients during a phase I/IIa clinical trial (Feron et al., 2005; Mackay-Sim et al., 2008). In addition, there is no associated co-morbidity since it has been shown that olfactory biopsies do not impair the sense of smell (Feron et al., 1998).

We have recently developed a cervical spinal cord contusion model relevant to the observed respiratory deficit after SCI (Baussart et al., 2006). This rat model induces a persistent, reproducible and quantifiable diaphragm respiratory deficit. It is a unique experimental model of high cervical contusion dedicated to assess the efficiency of cell transplantation on breathing recovery after cervical SCI. In the current study, we have tested whether a delayed transplantation of nasal OECs promote respiratory recovery. Functional recovery of breathing was assessed 3 months post-transplantation, using respiratory behavioural plethysmography and EMG of the diaphragm.

* Corresponding author. Université Paul Cézanne-CNRS UMR 6231, Avenue Escadrille Normandie Niemen, case 352, 13397 Marseille, France. Fax: +33 491 288 885.
[1] Equally contributing authors.

0014-4886/$ – see front matter © 2010 Elsevier Inc. All rights reserved.
doi:10.1016/j.expneurol.2010.07.002

Activity of phrenic nerve and immunohistochemistry were used to explore reorganizational changes in the cervical cord.

Materials and methods

Animal care and handling were conducted in accordance with the Guide for the Care and Use of Laboratory Animals, the Guidelines for the Use of Animals in Neuroscience Research and French laws relevant to animal experiments and surgery (accreditation no. C13-055-6 from the French Ministry of Agriculture).

Primary culture and purification of nasal OECs

Five male inbred Sprague Dawley adult rats, weighing 250 g, were used (Janvier, France). Cultures of OECs were prepared as previously described (Bianco et al., 2004; Lu et al., 2001). Briefly, the lamina propria was dissociated and cells were re-suspended in DMEM/HAMF12 supplemented with 10% foetal calf serum and plated on poly-L-lysine (2 μg/cm^2) coated dishes. Two days later, the culture medium was changed for serum-free medium supplemented with neurotrophin 3 (NT3, 50 ng/ml), which is known to enhance survival of OECs in culture with their purity approaching 100% (Bianco et al., 2004). Over 90% of cells in the OEC cultures were p75^{NFR} and GFAP immunoreactive. As a control for contamination with Schwann cells myelinating motor axons, cultures were tested and found negative with HNK1 antibody (Sigma Castle Hill, NSW, Australia). However, this testing could not rule out contamination with sensory axon-myelinating or non-myelinating Schwann cells, which are known to lack the HNK1 epitope (Bock et al., 2007; Martini et al., 1994; Saito et al., 2005)

Surgical procedures

Female adult Sprague Dawley rats, weighing 250 g at the start of the experiment, were used (Janvier, France). In order to avoid putative cell rejection, we used inbred littermates for both donor and receiver animals. Anesthesia was achieved intraperitoneally with pentobarbital (Nembutal, 50 mg/kg, ip; Sanofi, France). Cervical contusion was performed as previously described (Baussart et al., 2006) for contused control rats ($n=4$), MEDIUM and OEC rat groups ($n=6$ for each group). Briefly, through a midline dorsal cervical incision, a standard bilateral C2 laminectomy was performed with great care, especially when removing the left part of the vertebra, in order to visualize the far-lateral part of the left spinal cord. The dura was opened longitudinally and laterally at the level of the left C2 dorsal root (window of 2.5×2.5 mm) and a dorso-lateral resection of the pia matter was carried out with microscissors in order to remove a fragment measuring around 1 mm (transversal axis corresponding to the half-lateral part of the left C2 hemispinal cord)×1 mm (rostro-caudal axis). The aim of partly removing the pia matter was to reduce the shock absorption by the pia matter in order to intensify the damage on the ventrolateral white matter. The injury was performed caudally to the left C2 dorsal root under the operating microscope. A 0.8 mm-diameter, 120 mm-long metallic rod (referred as the impactor) was applied to the left C2 spinal cord at the level of the pia matter window and slowly lowered ventrally (3 mm depth) toward the floor of the C2 vertebral body. A 20 g weight was dropped along the impactor from a height of 12 cm. The compression was maintained for 30 min with the 20 g weight left *in situ*. Lastly, the impactor was removed gently, and the wound was closed without drainage after cleaning with betadine. This injury produces a persistent and reproductible hemi-diaphragm paralysis.

Cell transplantation

Fifteen days post-injury, rats were reanaesthetised with the same procedure as paragraph 2.2 and, after gaining surgical access to the injured region, cells or medium were transplanted using a 5 μl Hamilton glass syringe, connected to a 27 gauge needle and attached to a micromanipulator. MEDIUM animals received injection of DMEM/HAMF12, and transplanted animals received OECs. Medium or cells in the same medium were injected to the spinal cord on the site of the lesion. Injections were delivered at spinal sites 1.5 mm laterally from the midline: 1 mm rostrally, 1.5–2 mm caudally and inside the lesion. To reach the ventral and ventrolateral funiculi where the descending respiratory pathways are located, each spinal site received two injections (0.5 μl each) given at 2 and 3 mm below the dorsal surface of the cord. Each animal received a total of 6 injections (6×0.5 μl) which contained OEC suspension (100,000 cells/μl) or DMEM/HAMF12. The injection was given at 0.5 μl/min. The syringe was left in the injection site for 2 min to avoid reflux. No immunosuppressant was used.

Plethysmography

Ventilation was measured in awake unrestrained MEDIUM and OEC rats using barometric plethysmography. Control rats (uninjured) were used for comparison ($n=5$). According to the protocol described previously (Peyronnet et al., 2000), calibration of the chamber was obtained before placing the animal in the box. Either a MEDIUM or an OEC rat was placed in the chamber for measurements of ventilation. Tidal volume, respiratory frequency and minute ventilation were calculated from breath-by-breath over 30–50 consecutive cycles (around 30 s) by computer analysis of the spirogram. All measurements in normoxia were performed in quadruplet for each rat. The mean of these 4 values was considered as the basal ventilation. The hypoxic test was carried out by flushing the plethysmograph chamber with a mixture of 10% O_2 and 90% N_2. After the 10% O_2 level was reached inside the chamber, the system was clamped to perform the measurements (at 1, 4, 7 and 10 min after the beginning of hypoxia) of the hypoxic ventilatory response involving 40–60 breath cycles for each recordings. The mean of these 4 measurements represents ventilation in hypoxia.

Diaphragm electromyography

Three months post-grafting, the animals (300–400 g) were anesthetized and tracheotomized. Diaphragm electromyography (EMG) and integrated signal (Int EMG) activity of both right and left (ispilateral to the lesion) hemi-diaphragms were recorded as previously described (Polentes et al., 2004). The diaphragm EMG was studied during spontaneous breathing (eupnea) and during imposed hypercapnic conditions by adapting a 15 cm tube to the tracheal canula. End tidal CO2 was monitored using a check mate 9900 (PBI Dansensor) and ranged from 4.8% to 5.2% in eupnea to 7–7.5% during imposed asphyxic conditions in spontaneously breathing animals.

Phrenic nerves electrophysiology

After the EMG recordings, the animals were paralysed (neuromuscular blocking agent: Gallamine triethiodide, 10 mg/kg, iv; Rhône-Poulenc Rorer, France) and ventilated. Spontaneous activity of both left (ipsilateral to the lesion) and right phrenic nerves were recorded (phrenic neurogram, PN; integrated PN, int PN) as previously described (Polentes et al., 2004) during eupnea and hypercapnia.

The spinal cord connectivity was tested using phrenic orthodromic activation elicited by supralesional spinal cord stimulation (tungsten bipolar electrodes: Frederik Haer, 10 kΩ) of the C1 ventral and ventrolateral funiculi, as previously described (Gauthier and Monteau, 1986; Polentes et al., 2004). These spinal areas include descending respiratory bulbo-spinal axons which form monosynaptic connections with phrenic motoneurons (Lipski et al., 1994; Speck, 1988).

Acute sections at the C1 cervical level were conducted at the end of this invasive surgery/electrophysiology procedure only if the healthy

state (EKG, temperature, myosis) of the animal was stable since transcardiac perfusion was necessary for immunohistochemistry. In each condition, 3 animals did not respond to these healthy criteria and were thus excluded from acute sections and directly perfused.

All signals were monitored on a Gould oscilloscope (Gould 1604) and computer recorded using the Gould Transition software (Designed by P. Sanchez, CNRS).

Quantitative aspects of diaphragm and phrenic nerve activity

Twelve different recording sites were used to study the EMG activity of each hemi-diaphragm. To evaluate the degree of activity of the left diaphragm, ipsilateral to the spinal injury, the area of each rectified and integrated trace under the diaphragm EMG was calculated using a software specifically designed (Dr. P. Sanchez, CNRS) to exclude any deflection of the rectified and integrated traces due to artefactual incidence, such as deflections due to EKG in sites near the heart. The 12 recording sites cover a substantial area of the parts of the muscle involved in breathing activity, that is, the pars sternalis, the rostral pars costalis and the rostral part of the lumbar diaphragm which surrounds the level of the cava vein. For each recording site, the averaged area of five characteristic successive EMG rectified and integrated traces was calculated. For each recording site, the left averaged rectified and integrated area was calculated as a percentage of the corresponding right rectified and integrated surface (% left/right). For each animal, the mean left EMG diaphragm activity

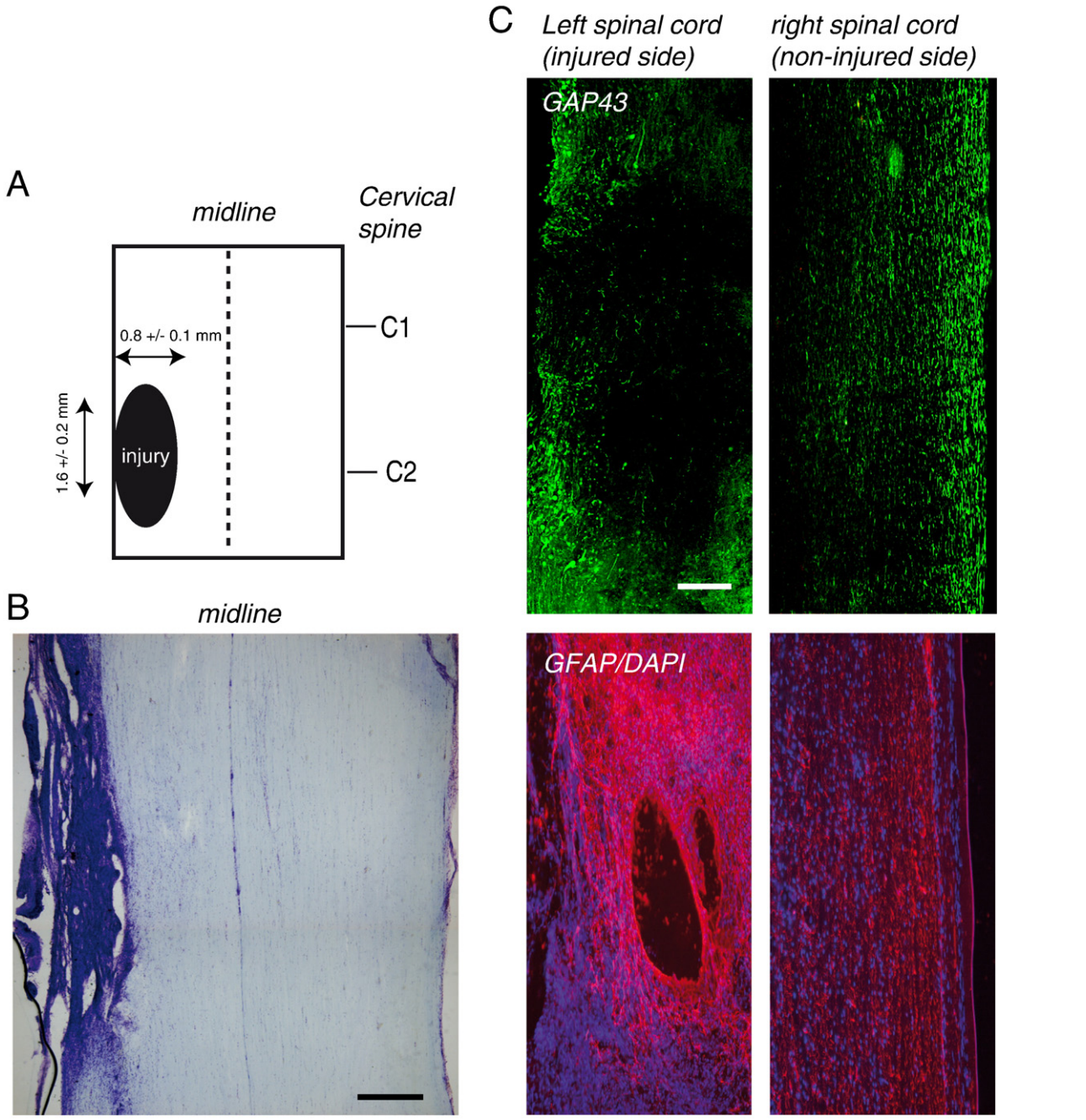

Fig. 1. Histological representation of a lateral compression/contusion of the rat spinal cord at the C2 cervical level. **A:** Drawing represents a longitudinal view of the cervical spinal cord with the injury indicated by a large black dot. The size of the injury was measured 3 months post-injury. **B:** Violet cresyl on longitudinal/horizontal section was performed 3 months post-injury to show the extent of the lesion at the ventral level (scale bar: 500 μm). **C:** Immunocytochemistry for GAP43 and GFAP was performed 2 days post-injury on longitudinal/horizontal sections of the cervical spinal cord (scale bar: 200 μm).

was calculated as the average of the 12 recording sites (% left/right). To quantify the activity of the left phrenic nerve ipsilateral to the lesion, five successive typical phrenic bursts were selected and the average surface of their rectified and integrated traces was calculated using the same software as for diaphragm EMG. For each rat, and for each step of the experiment, the left averaged rectified and integrated phrenic nerve activity was calculated as a percentage of the corresponding right rectified and integrated surface (% left/right). In each animal, the right phrenic nerve activity was taken as a reference to quantify the left one under chronic conditions, to prevent inter-variability.

Immunohistochemistry

Longitudinal/horizontal sections of the cervical spinal cord of 30 μm were cut on a cryostat. Following two rinses in 0.1 M PBS, sections on slides were permeabilized using 0.1 M PBS containing 0.2% Triton X-100 for 30 min. Sections were pre-incubated for 1 h in 0.1 M PBS containing 4% of goat serum and incubated overnight at 4 °C with the corresponding primary antibody: rabbit anti-serotonin (1/2000, Sigma, USA), mouse anti-neurofilament H phosphorylated (1/1000, Eurogentec-Covance, USA), rabbit anti-GFAP (1/1000; DAKO, France), and rabbit anti-GAP43 (1/1000; Chemicon, USA). Following primary antibody incubation, sections were incubated 1 h at room temperature with the appropriate secondary antibody: goat anti-mouse Alexa 488 and goat anti-rabbit Alexa 594 (1/400; Invitrogen, France).

Image analyses

Confocal images were captured with a Leica TCS SP2 scanning confocal microscope (Leica) equipped with a 10× lens (HCX PL APO, NA 0.4), argon (488 nm) and helium (543 nm) lasers and monitored with LCS v2.61 image acquisition software. On longitudinal/horizontal sections, Z-stacks from 10 confocal images (1 μm focal spacing) were acquired at the C2 level where the lesion site was visualized by the GFAP-reactive border. For all animals in each treatment group, confocal images were performed in the ipsilateral (injured side) and the corresponding contralateral part (uninjured side). Confocal images were initiated dorsoventrally, 0.5 mm above the vertebral floor, and mediolaterally, from the most lateral part of the white matter to the most lateral part of the ventral horn. Neurofilament and serotonin immunodensitometry were performed using ImageJ (NIH software). Quantification of neurofilament and serotonin pixels within the lesion site was performed by outlining areas measuring 790,000 pixels, splitting RGB channels to conserve neurofilament and serotonin pixels. Images were converted to 8 bit type images, binary processed and a similar threshold was applied to normalize staining between animals. Limit to threshold was checked to include in measurement calculations only thresholded pixels. Number of neurofilament and serotonin positive pixels were then counted using the measure tool of ImageJ software.

Results

In order to injure the respiratory bulbo-spinal descending pathways that control the phrenic motoneuron discharges, all rats received a lateral contusion on the left side of the spinal cord at the C2 cervical level. The efficiency of the contusion was verified using contused control rats (Fig. 1). Immunoreactivity of GAP-43 confirmed that 48 h after injury, nerve fibers of the spinal cord were injured on the ipsilateral side (injured side) while the controlateral side (non-injured) remained intact. As a constituent of astrocytes, GFAP immunoreactivity was detected in non-injured side of the cord, but GFAP immunoreactivity was upregulated on the injured side indicating the presence of classical astrocyte reactivity after injury. Fifteen days after injury, nasal OEC cells were transplanted in the injured side in one animal group (stated as OEC, $n=6$) while the other group received volume-matched DMEM injection (stated as MEDIUM, $n=6$). We then assessed the animals 3 months post-transplantation.

Functional partial recovery of breath behavior

To avoid weight-dependent variations in breathing patterns (Fuller et al., 2008), Control (uninjured), MEDIUM and OEC rat groups were weight-matched (Control: 0.302 ± 0.011; MEDIUM: 0.312 ± 0.013; OEC: 0.325 ± 0.028 kg). Three and half months post-injury, plethysmography analyses revealed that, in normoxia (i.e. 21% O_2, balance N_2), injured animals (either MEDIUM or OEC) had lower minute ventilation values compared to control rats. Moreover, both MEDIUM and OEC groups had similar minute ventilation values (Fig. 2A). In contrast, during hypoxia

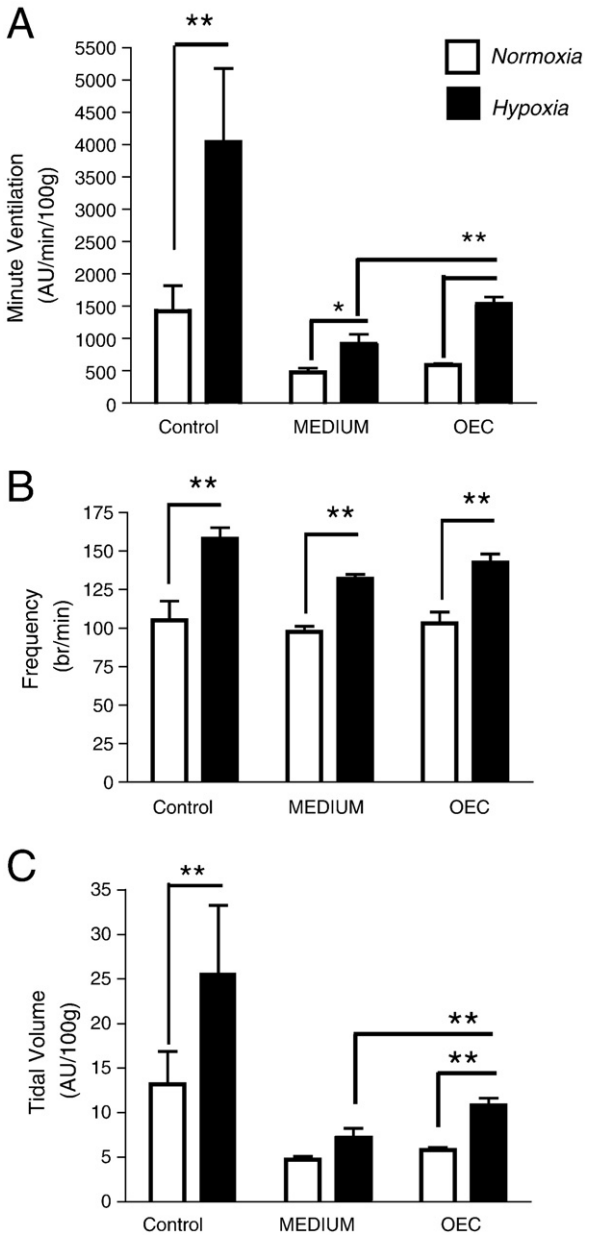

Fig. 2. Breathing performance of control (uninjured), MEDIUM and OEC-grafted rats 3.5 months post-contusion. Minute ventilation (A), inspiratory frequency (B) and tidal volume (C) were recorded during quiet breathing (normoxia) and hypoxia (10% O_2). Statistical comparisons were performed using a two-way ANOVA test. Control ($n=5$); MEDIUM and OEC ($n=6$). Error bars represent SEM. *: p value < 0.05; **: p value < 0.01.

(10% O_2, balance N_2), breathing values in OEC-transplanted rats were significantly greater than in MEDIUM (Fig. 2A). In order to define which respiratory volume parameters could be responsible for this breath behavior benefit, we analyzed the frequency and tidal volume breathing of the two groups (Fig. 2B and C). In normoxia condition, both groups had similar breathing frequency and tidal volume. In contrast, OEC-transplanted rats responded to hypoxia with an increase in tidal volume while breathing frequency was unaffected.

Nasal olfactory ensheathing cells transplantation promotes diaphragm partial recovery

The observed improvement of breathing behavior after OEC transplantation led us to evaluate the spontaneous muscular activity of the diaphragm, 3 months post-transplantation (Fig. 3). The frequency of the EMG cycles recorded bilaterally was the same in both groups of animals. These findings were consistent with those reported above, using plethysmography. However, while the right-hemi-diaphragm (non-injured side) remained completely active with no difference between MEDIUM and OEC groups, the left hemi-diaphragm (injured side) of the MEDIUM group had a weaker activity, when compared to that of the OEC groups (Fig. 3A). We observed that $21 \pm 7\%$ of the injured hemi-diaphragm remained spontaneously active compared to the right hemi-diaphragm of MEDIUM group. However, in the OEC group, activity of the injured hemi-diaphragm was significantly increased to $51 \pm 6\%$ (Fig. 3B). This significant increased in OEC compared to MEDIUM group, in normoxic condition (p value $= 0.025$), was also observed during hypercapnia conditions (OEC: $73 \pm 7\%$; MEDIUM: $36 \pm 11\%$; p value $=$ 0.0286). As a result, the OEC-related improved breathing function originated from a recovery of the left hemi-diaphragm, ipsilateral to the injured cervical cord.

Transplantation of nasal olfactory ensheathing cells promotes partial recovery of the left phrenic nerve activities

To further assess the effects of nasal OEC transplantation in SCI rats, we recorded the spontaneous electrophysiological activities of both the left (injured) and right (uninjured) phrenic nerves (Fig. 4A). In both MEDIUM and OECs rat groups, spontaneous activities of the left and right nerves were present. The right phrenic nerve activities of both groups appeared similar since no difference between the averaged surfaces of the phrenic nerve integrated traces were detected. However, as a consequence of the left lateral contusion, the left phrenic nerve activities were always weaker than the right ones. We found that, in the MEDIUM rats, the left phrenic nerve exhibited an activity average of $23 \pm 4\%$ as compared to the right one. In the OEC group, the activity rose to $54 \pm 3\%$. Thus, the increase in the OEC rats was significantly greater than that in the MEDIUM group (Fig. 4B). These results confirm the functional partial recovery of the diaphragm following the OEC transplantation.

We next investigated the spinal origin of the left phrenic nerve activity (Fig. 4C). After lateral left contusion, the left phrenic nerve activity observed in Fig. 4A could arise from the contralateral (uninjured) spinal cord due to the compensatory "Crossed Phrenic nerve Phenomenon" (CPP) (Goshgarian, 2003) and/or from ipsilateral (injured) spinal cord due to a recovery of the ipsilateral descending respiratory pathways. To explore these two hypotheses, we performed supralesional spinal cord stimulation at the C1 cervical level. In both MEDIUM and OEC rats, typical orthodromic right phrenic responses were obtained by stimulating the ventrolateral column of the right C1 cervical spinal cord (Fig. 4C, right panels). No statistical differences were observed when comparing the latency and the amplitude of these responses between two groups. However, when the stimulation was applied to the ventrolateral column of the left C1 cervical spinal cord, we observed a lack of response of the left phrenic nerve in the MEDIUM group (Fig. 4C, left panel). Stimulation extended to other left C1 spinal cord areas (lateral, latero-dorsal and ventral columns) also did not elicit response on the left phrenic nerve (not illustrated). This result demonstrated that, in the MEDIUM group, spontaneous activities of the left phrenic nerve, and thus the left hemi-diaphragm were not arising from a recovery of the ipsilateral descending pathways but most probably it was due to CPP. In contrast, in the OEC group, stimulation of the ventrolateral column of the left C1 cervical spinal cord produced orthodromic left phrenic responses with an increased latency and lower amplitude than that obtained on the controlateral right side (Fig. 4C, left panel).

Partial recovery of the left phrenic nerve promoted by nasal olfactory ensheathing cells is mediated by restoration of ipsilateral supraspinal command

To confirm and further explore the origin of the left phrenic nerve activity that was observed at 3.5 months after ipsilateral trauma, we performed, under anesthesia and artificial ventilation conditions, an acute section at the C1 cervical level (Fig. 5). In each case, the section started from the midline to the right lateral part of the cord along its entire depth and the effect of the progressive section on the activity of both phrenic nerves was continuously recorded. In the OEC group, the section was also applied from the midline to the left lateral part.

We found that in MEDIUM rats, (Fig. 5A), a medial right section was enough to completely abolish the left phrenic activity and to induce a strong decrease of the right phrenic discharge (Fig. 5A, trace 2). The right activity was then totally abolished when the section was prolonged laterally (complete C1 right hemisection) (Fig. 5A, trace 3). The fact that any left phrenic activity subsisted after right C1 hemisection (which interrupts descending right command and particularly the pathways potentially involved in the CPP) confirmed that the left phrenic activity of the MEDIUM rats originated from the compensatory effect of the CPP. In contrast for OEC rats, the medial right section had only poor effect on the left phrenic nerve activity (Fig. 5B, trace 2). This activity was only partially abolished after C1 right hemisection (Fig. 5B, trace 3) and around half of the activity persisted (53%; Fig. 5C). Like in MEDIUM rats, the right phrenic nerve activity was completely suppressed after the rostral ipsilateral hemisection (Fig. 5B, trace 2). Total interruption of the left phrenic nerve activity in OEC rats was exclusively obtained after a complete C1 acute section (when the section was directed toward the left side) (Fig. 5B, trace 4).

Transplantation of nasal olfactory ensheathing cells promotes axonal sprouting into the lesion site

We finally investigated, at the anatomical level, how OEC transplantation partially restored the ipsilateral command. For that purpose, we performed longitudinal sections throughout the contusion site and assessed the presence of axons, using the GFAP-positive border to delineate the boundaries of the contusion site. Densitometry of neurofilament (NF) and 5-HT axon fibers was performed by counting NF and 5-HT pixels within the area of the contusion site (Fig. 6). In the MEDIUM group, the rostral, epicenter and caudal sites

Fig. 3. Diaphragm activities of MEDIUM and OEC-grafted rats 3.5 months post-contusion. **A** and **B:** Typical EMG activity of left and right hemi-diaphragm in MEDIUM and OEC-transplanted rats, during spontaneous breathing (normoxia) and imposed asphyxic (hypercapnia) conditions, is reported. Each hemi-diaphragm activity includes both the diaphragm trace (EMG) and the integrated trace (EMG Int). **C:** Bar graphs, report diaphragm activity in normoxia and hypercapnia conditions ($n = 6$). Statistical comparisons were performed using a Student's t-test. Error bars represent SEM. *: p value < 0.05

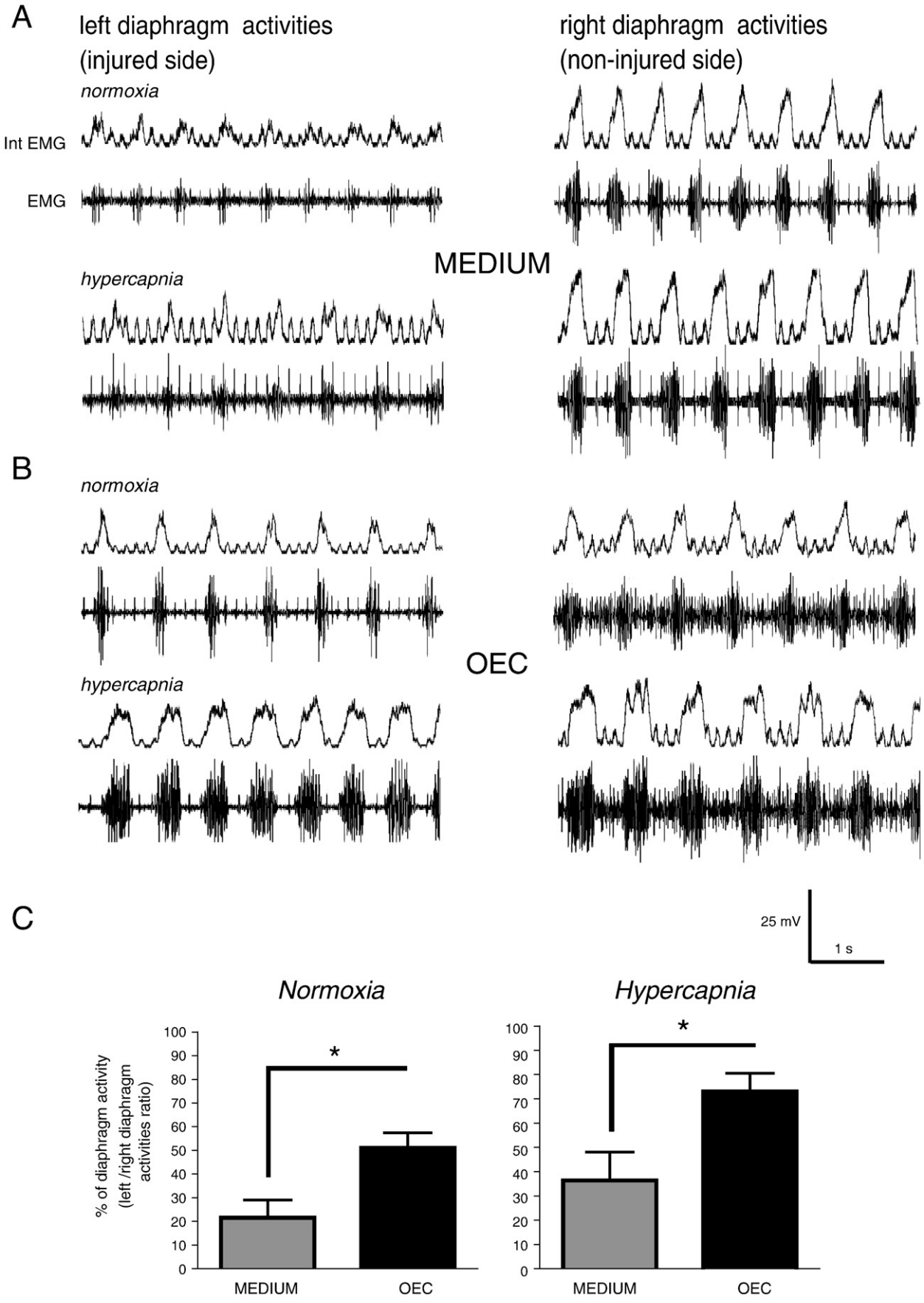
A
left diaphragm activities
(injured side)
right diaphragm activities
(non-injured side)
normoxia
Int EMG
EMG
MEDIUM
hypercapnia
B
normoxia
OEC
hypercapnia
25 mV
1 s
C
Normoxia
Hypercapnia
% of diaphragm activity
(left /right diaphragm
activities ratio)
100
90
80
70
60
50
40
30
20
10
0
*
MEDIUM
OEC

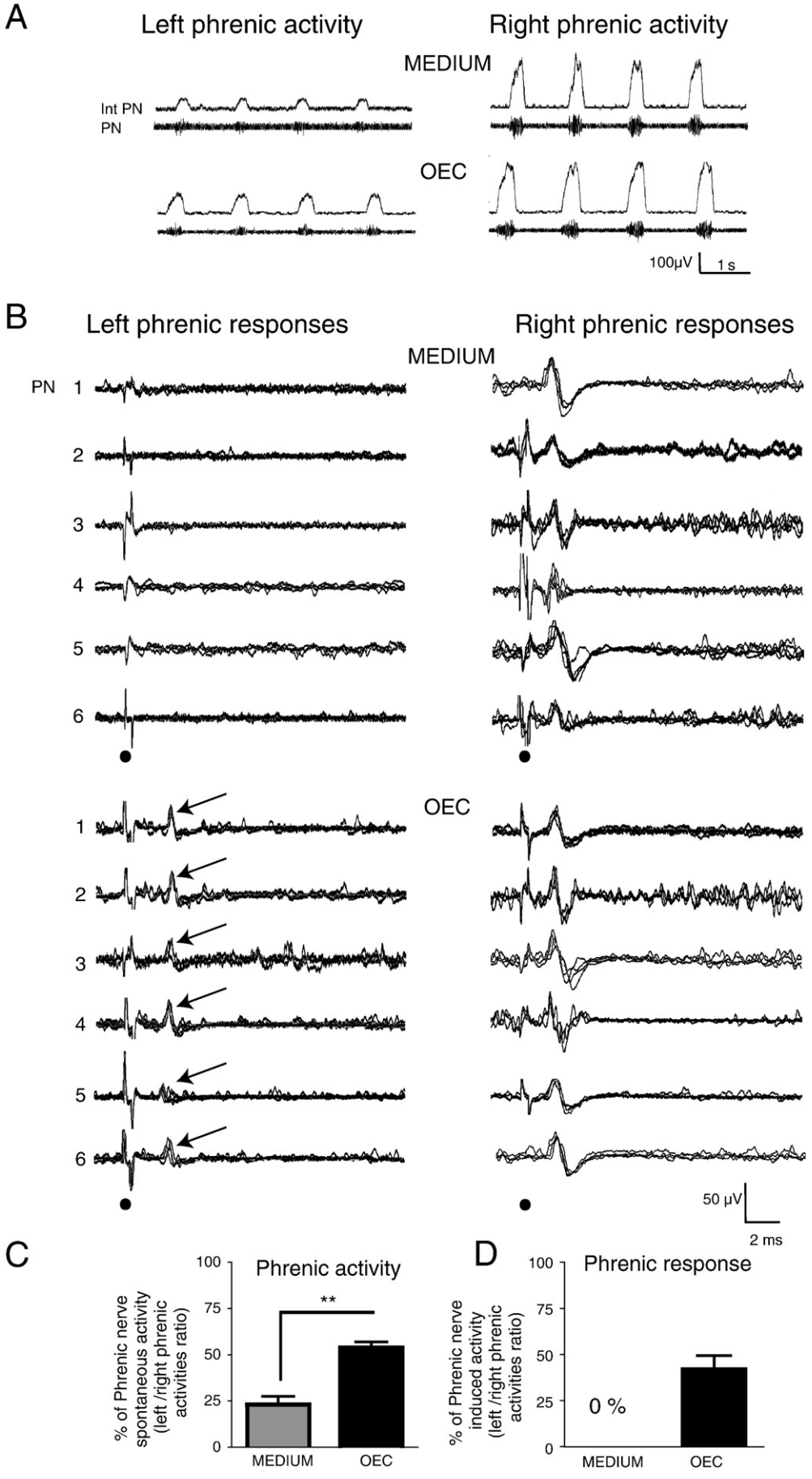
A
Left phrenic activity
Right phrenic activity
MEDIUM
Int PN
PN
OEC
100µV
1 s
B
Left phrenic responses
Right phrenic responses
MEDIUM
PN 1
2
3
4
5
6
OEC
1
2
3
4
5
6
50 µV
2 ms
C
Phrenic activity
% of Phrenic nerve spontaneous activity (left /right phrenic activities ratio)
100
75
50
25
0
**
MEDIUM
OEC
D
Phrenic response
% of Phrenic nerve induced activity (left /right phrenic activities ratio)
100
75
50
25
0
0 %
MEDIUM
OEC

of the contusion were almost devoid of axons (Fig. 6A), as observed 48 h after the contusion (Fig. 1). The small number of bouton-like varicosities of 5-HT immunoreactive fibers was seen preferentially in the epicenter of the contusion site (Fig. 6B). As previously observed by other groups (Ramer et al., 2004; Richter et al., 2005), we found that 3.5 months post-injury, OEC transplantation reduced cystic cavity area (Fig. 6C). This reduction of cavity area reduction was paired with a significant increase in NF-positive and 5-HT axons of currently unknown sources that were promoted by OECs when compared to MEDIUM rats (Fig. 6D and E). Neurofilament-positive fibers were mainly orientated in a rostro-caudal way, both in the ventrolateral and ventromedial aspects. As expected, unaffected ventrolateral neuronal fibers were observed in the white matter of the contralateral side. Bouton-like varicosities of 5-HT immunoreactive fibers were present throughout the contusion site. However, no evidence of 5-HT-positive cell bodies was observed. Finally, both neurofilament and 5-HT-positive axons were found in large number rostral to and within the lesion site and in small number in the caudal area.

Discussion

In line with the pioneering studies of Ramón-Cueto and Nieto-Sampedro (Ramon-Cueto and Nieto-Sampedro, 1994; Ramon-Cueto et al., 1998), numerous reports have demonstrated the therapeutic benefit of OECs when transplanted in rodent models of spinal cord injury (Richter and Roskams, 2008). However, most of these models, based on straight hemi- or total transection of the thoracic dorsal columns, do not accurately reflect the type of injury – contusion or elongation – usually observed in humans (Bohlman and Anderson, 1992). Furthermore, the vast majority of studies elected a thoracic section as their preferred model while epidemiology indicates that more than 50% of SCIs in humans results from a cervical trauma (Jackson et al., 2004). Finally, most studies have chosen to acutely transplant OECs, precluding therefore the possibility to perform autologous graftings. Interestingly, the team that conducted the first clinical trial based on the use of nasal OECs, opted for autologous transplants in chronically injured paraplegic patients (Feron et al., 2005). Three years post-implantation, the procedure was evaluated as feasible and safe (Mackay-Sim et al., 2008).

The present study is the first to assess the respiratory benefit of nasal OECs, when subchronically grafted in a rat model of cervical contusion. Furthermore, in harmony with the protocol used in the reported clinical trial, we chose to perform semi-autologous (same litter-mate) graft of nasal OECs in a subchronic model of SCI. In addition, in order to be as close as possible to clinical context, we elected a cervical contusion inducing a persistent unilateral diaphragmatic paralysis (Baussart et al., 2006). Finally, we transplanted OECs after a 2-week delay when a peak in reactive astrocyte response is observed (Tian et al., 2007). Therefore, we were able to assess OECs efficiency during glial scarring. As a result, this study is the first to assess the respiratory benefit of nasal OECs, when subchronically grafted in a rat model of cervical contusion.

We found that there was a significant difference in the response to hypoxia between the MEDIUM and OEC groups: the hypoxia-induced increase in minute ventilation was greater in the OEC than MEDIUM rats. Similar minute ventilation during normoxia in both groups of rats is in an agreement with (Fuller et al., 2008) who reported that cervical hemisection does not impair basic levels of ventilation despite of persisting chronic injury. However, the capacity of an injured rat to maintain basic levels of ventilation and to respond to increased respiratory drive are highly dependent of the CPP (Fuller et al., 2008; Golder et al., 2003). Here, we confirm that, 3.5 months post-injury, basic levels of ventilation in injured rats (MEDIUM group) rely exclusively on the CPP as an acute contralateral hemisection completely abolishes ipsilateral phrenic rhythmic output. CPP is also at play in the OEC group but is not the unique component since the acute contralateral hemisection did not abolish the ipsilateral phrenic rhythmic output. In the OEC group, persistent spontaneous activities of both the ipsilateral phrenic nerve and the diaphragm and their response to hypercapnia indicate that OECs may restore, at least partially, the injured phrenic input.

Functional electrophysiology findings also support a role of OECs in the re-establishment of the ipsilateral injured phrenic central command. First, supralesional stimulation (at C1 level) elicited sub-lesional ipsilateral postsynaptic phrenic responses in the OEC group and not in the MEDIUM group. Second, the spontaneous ipsilateral phrenic rhythmic activity which was maintained after an acute C1 contralateral hemisection was completely abolished only when an acute ipsilateral C1 hemisection was performed, thus attesting of the involvement of ipsilateral pathways restoration in maintaining phrenic activity after contralateral lesion. However we cannot exclude that the partial recovery seen after OEC transplants could arise from a contralateral path that sprouts to the injured side above the level of the acute C1 contralateral hemisection.

Anatomical data are also consistent with the observed respiratory recovery. Spinal cord contusion clearly induced a dramatic loss of axons within and at the boundaries of the injury site. In contrast, rostro-caudal transplantation of nasal OECs enhanced axonal re-growth. This observed axogenesis is in line with previous studies describing the hypertrophic response of OECs on axonal regrowth (Raisman and Li, 2007). For example, it is known that OECs i) inhibit hypertrophic response of host astrocyte (Santos-Silva et al., 2007), ii) reduce the expression of chondroitin sulfate proteoglycans (CSPG) in reactive astrocytes (Lakatos et al., 2000), iii) limit the size of cavities (Richter et al., 2005), iv) create a tube-like structure and provide a bridge for lesioned axons (Li et al., 2004; Sasaki et al., 2004), and v) enhance angiogenesis (Richter et al., 2005). In line with these previously published data on the consequences of OECs grafting, we found here that nasal OECs reduce cystic size cavities which probably could create a bridge and thus could enhance axonal regrowth. Altogether, these studies demonstrate that OECs, from bulbar or nasal origin, provide a positive environment for injured axons probably by regulating the cellular and molecular events forming the glial scar. To date, there is no a single antigen recognized as an unambiguous marker of this cell type. As a consequence, it was not possible to ascertain that our cultures were free of other cell types. We have shown that, in our culture conditions, we were able to get pure populations (up to 98%) of cells expressing GFAP and S100 (Bianco et al., 2004). Nevertheless, it cannot be excluded that some of the stem cells residing in the lamina propria (Delorme et al., 2010), which may express these two proteins, were present in our culture dishes.

In order to assess survival and migration of transplanted cells, we permanently transfected them with the gene coding for the fluorescent protein GFP, using a lentivirus. As routinely observed in our lab with human cells (Delorme et al., 2010), about half of the rat cells were successfully transfected, after 1 day in the appropriate culture medium. However, a few days later, we observed that GFP expression was transient and we could not get high numbers of cells

Fig. 4. Spontaneous and evoked phrenic nerve activities of MEDIUM and OEC-grafted rats 3.5 months post-contusion. **A:** Typical phrenic activity in MEDIUM and OEC-transplanted rats is reported. Each phrenic nerve activity includes the spontaneous trace (PN) and the integrated trace (Int PN). **B:** Typical left and right phrenic responses from four MEDIUM and OEC animals evoked by supralesional stimulation (single pulse; 500 μs, 0.4 mA), applied on the left and right side of the spinal cord (C1 level), respectively. In each trace, 4 superimposed individual traces are represented. Dots indicate stimulation; arrowheads indicate responses of OEC left phrenic responses. **C** and **D:** Bar graphs indicate the level of phrenic recovery by quantifying spontaneous activity ($n=6$) (C) or induced activity ($n=6$) (D). Left phrenic nerve activity normalised to the right phrenic nerve activity. Statistical comparison was performed using a Student's *t*-test. Error bars represent SEM. **: p value <0.01.

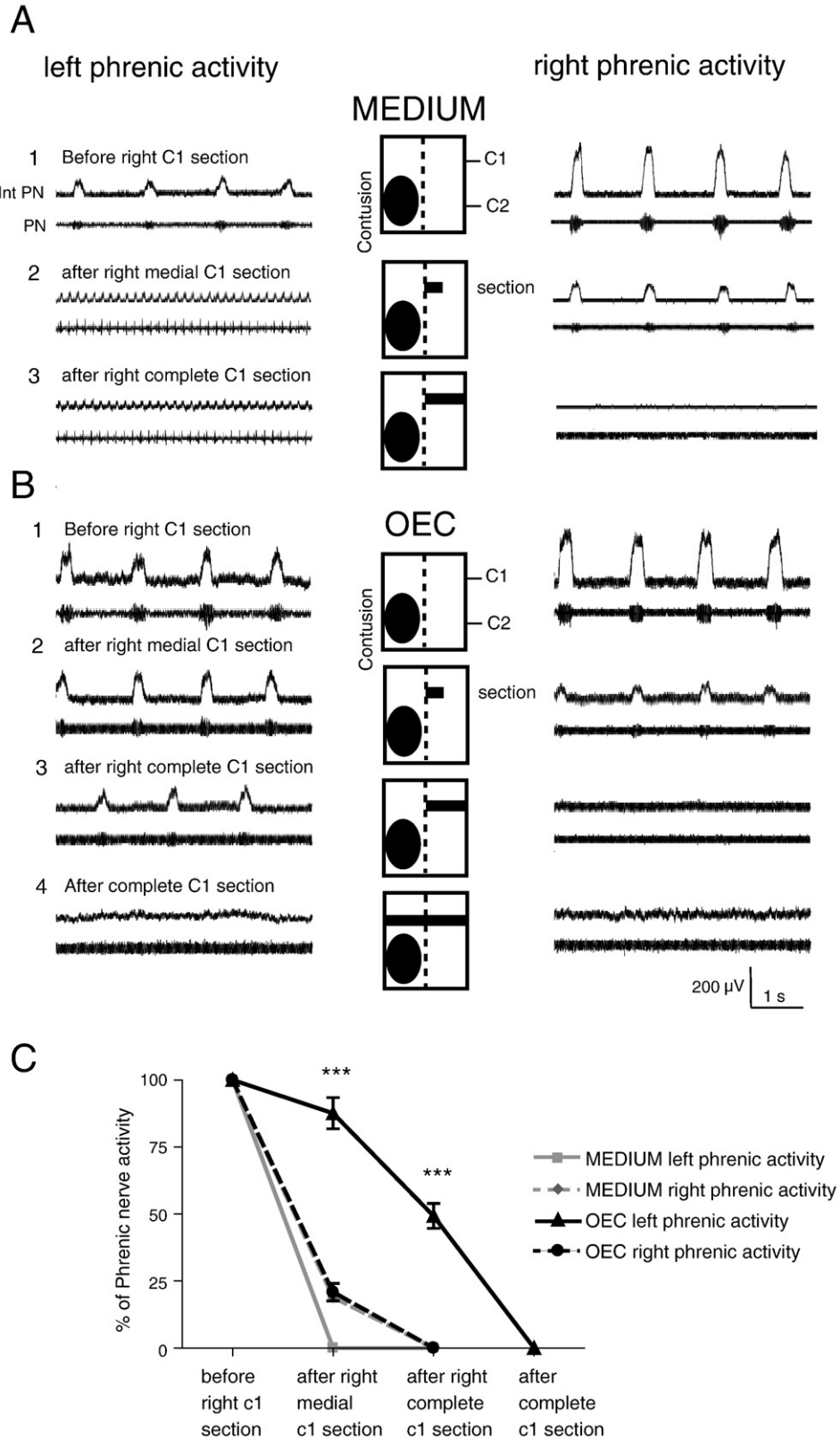

Fig. 5. Effect of acute additional sections on phrenic nerve activities of MEDIUM and OEC-grafted rats 3.5 months post-contusion. **A** and **B:** Typical phrenic spontaneous activity in MEDIUM (A) and OEC-transplanted rats (B), before and after acute sections, is reported. Each phrenic nerve activity includes the spontaneous trace (PN) and the integrated trace (Int PN). The drawing represents a dorso-longitudinal view of the cervical spinal cord, with the contusion injury site indicated by a large black dot and the horizontal black line represents the extent of C1 acute sections (contralateral right medial, right complete or complete section). **C**: Plot graph reports the remaining right and left nerve activities of MEDIUM and OEC-transplanted rats, after various acute C1 sections ($n=3$). Statistical comparison was performed using a two-way ANOVA test. Error bars represent SEM. **: p value <0.01.

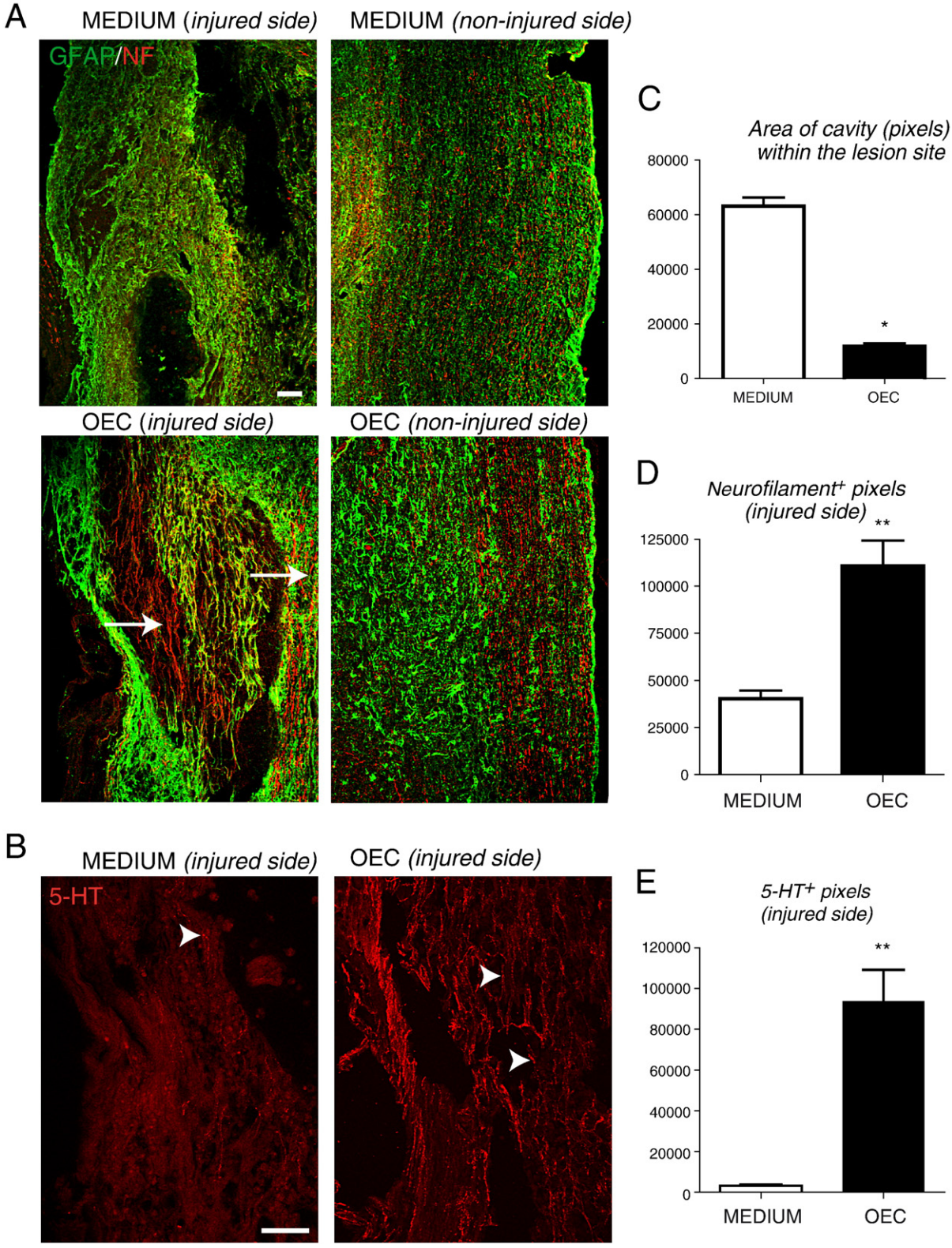

Fig. 6. Assessment of axon sprouting within the lesion site 3.5 months post-contusion. **A**: Longitudinal sections were immunostained with anti-GFAP and anti-neurofilament (NF) antibodies. Views of ipsilateral (injured side) and corresponding contralateral (non-injured) sides indicate that neuronal fibers are detected in the ventrolateral and ventromedial part of the spinal cord of OEC-grafted rats (arrows) and not in MEDIUM animals. **B**: Longitudinal sections were immunostained with anti-5-HT antibody. High numbers of 5-HT-positive axons with varicosities (arrowheads) were found in the OEC group, when compared to the MEDIUM group. Scale bar: 100 μm. **C**: The area of cystic cavity formed after injury is significantly reduced after OEC transplantation ($n=4$; *: p value<0.05). **D** and **E**: Fluorescence densitometries for NF-positive (D) and 5-HT-positive (E) pixels, within the lesion site, reveal significantly greater NF and 5-HT immunoreactivity after OEC transplantation ($n=4$; **: p value<0.01). Data are presented as mean ± SEM.

with a stable GFP expression before transplantation. We think that the lentiviral vector itself was not packaged properly or has not integrated the genome

In regard to locomotor recovery after SCI, it is worth mentioning that several studies have reported an increase of 5-HT immunoreactive axons following engraftment of OEC or embryonic cells (Fouad et al., 2005; Lopez-Vales et al., 2006; Lopez-Vales et al., 2007; Lu et al., 2001; Ramon-Cueto et al., 1998; Richter et al., 2005). These results suggest a regeneration of the raphe-spinal pathway. Some studies report that 5-HT-positive axons and occasionally interneurons can be found in the caudal stump after a spinal cord section (Kubasak et al., 2008; Newton et al., 1986; Takeoka et al., 2009). In our contusion model, we failed to detect 5-HT cell bodies or immunoreactive axons crossing the midline of the spinal cord. However, in the OECs rats, immunoreactive axons were found to be rostro-caudally oriented, with a high number of fibers in the rostral stump within the contusion site. These findings support the hypothesis that OECs would not necessarily contribute to the remodeling of propiospinal 5-HT interneurons but would rather induce central pathway regeneration and/or non-injured descending axons sprouting.

Such a central descending pathway reorganization could originate from 5HT raphe-spinal neurons which are known to directly innervate phrenic motoneurons and participate in respiratory plasticity during intermittent hypoxia (Baker-Herman et al., 2004; Dobbins and Feldman, 1994).

In conclusion, the current study provides, for a specific motor function (respiration), new evidence that nasal OEC transplantation can induce a partial recovery of respiratory function of the diaphragm following an injury of the cervical cord. Our results could have clinical implications as a potential treatment of the ventilator-dependent tetraplegic patients.

Acknowledgments

This work was supported by a grant from the Centre National de la Recherche Scientifique (CNRS), the Institute pour la Recherche sur la Moelle Epinière et l'Encéphale (IRME, Paris, France), Association Française contre les Myopathies (AFM, Paris, France) and Paul Cézanne University (Marseille, France). M.S. Félix was supported by a fellowship from the French Minister for Research and Technology. We thank the imaging facility of the Institut Français de Recherche Jean Roche and Patrick Sanchez (CNRS, France) for software design. The authors gratefully acknowledge Dr. Teresa Trippenbach (McGill University, Canada) for her helpful advice and critical review of the manuscript.

References

Baker-Herman, T.L., Fuller, D.D., Bavis, R.W., Zabka, A.G., Golder, F.J., Doperalski, N.J., Johnson, R.A., Watters, J.J., Mitchell, G.S., 2004. BDNF is necessary and sufficient for spinal respiratory plasticity following intermittent hypoxia. Nat. Neurosci. 7, 48–55.

Baussart, B., Stamegna, J.C., Polentes, J., Tadie, M., Gauthier, P., 2006. A new model of upper cervical spinal contusion inducing a persistent unilateral diaphragmatic deficit in the adult rat. Neurobiol. Dis. 22, 562–574.

Berlly, M., Shem, K., 2007. Respiratory management during the first five days after spinal cord injury. J. Spinal Cord Med. 30, 309–318.

Bianco, J.I., Perry, C., Harkin, D.G., Mackay-Sim, A., Feron, F., 2004. Neurotrophin 3 promotes purification and proliferation of olfactory ensheathing cells from human nose. Glia 45, 111–123.

Bock, P., Beineke, A., Techangamsuwan, S., Baumgartner, W., Wewetzer, K., 2007. Differential expression of HNK-1 and p75(NTR) in adult canine Schwann cells and olfactory ensheathing cells in situ but not in vitro. J. Comp. Neurol. 505, 572–585.

Bohlman, H.H., Anderson, P.A., 1992. Anterior decompression and arthrodesis of the cervical spine: long-term motor improvement. Part I–Improvement in incomplete traumatic quadriparesis. J. Bone Joint Surg. Am. 74, 671–682.

Brown, R., DiMarco, A.F., Hoit, J.D., Garshick, E., 2006. Respiratory dysfunction and management in spinal cord injury. Respir. Care 51, 853–868 discussion 869-870.

Delorme, B., Nivet, E., Gaillard, J., Haupl, T., Ringe, J., Deveze, A., Magnan, J., Sohier, J., Khrestchatisky, M., Roman, F.S., Charbord, P., Sensebe, L., Layrolle, P., Feron, F., 2010. The human nose harbors a niche of olfactory ectomesenchymal stem cells displaying neurogenic and osteogenic properties. Stem Cells Dev. 19, 853–866.

Dobbins, E.G., Feldman, J.L., 1994. Brainstem network controlling descending drive to phrenic motoneurons in rat. J. Comp. Neurol. 347, 64–86.

Feron, F., Perry, C., McGrath, J.J., Mackay-Sim, A., 1998. New techniques for biopsy and culture of human olfactory epithelial neurons. Arch. Otolaryngol. Head Neck Surg. 124, 861–866.

Feron, F., Perry, C., Cochrane, J., Licina, P., Nowitzke, A., Urquhart, S., Geraghty, T., Mackay-Sim, A., 2005. Autologous olfactory ensheathing cell transplantation in human spinal cord injury. Brain 128, 2951–2960.

Fouad, K., Schnell, L., Bunge, M.B., Schwab, M.E., Liebscher, T., Pearse, D.D., 2005. Combining Schwann cell bridges and olfactory-ensheathing glia grafts with chondroitinase promotes locomotor recovery after complete transection of the spinal cord. J. Neurosci. 25, 1169–1178.

Fuller, D.D., Doperalski, N.J., Dougherty, B.J., Sandhu, M.S., Bolser, D.C., Reier, P.J., 2008. Modest spontaneous recovery of ventilation following chronic high cervical hemisection in rats. Exp. Neurol. 211, 97–106.

Gauthier, P., Monteau, R., 1986. Respiratory resetting induced by activation of inspiratory bulbo-spinal neurons. Respir. Physiol. 65, 155–168.

Golder, F.J., Fuller, D.D., Davenport, P.W., Johnson, R.D., Reier, P.J., Bolser, D.C., 2003. Respiratory motor recovery after unilateral spinal cord injury: eliminating crossed phrenic activity decreases tidal volume and increases contralateral respiratory motor output. J. Neurosci. 23, 2494–2501.

Goshgarian, H.G., 2003. The crossed phrenic phenomenon: a model for plasticity in the respiratory pathways following spinal cord injury. J. Appl. Physiol. 94, 795–810.

Jackson, A.B., Dijkers, M., Devivo, M.J., Poczatek, R.B., 2004. A demographic profile of new traumatic spinal cord injuries: change and stability over 30 years. Arch. Phys. Med. Rehabil. 85, 1740–1748.

Kocsis, J.D., Lankford, K.L., Sasaki, M., Radtke, C., 2009. Unique in vivo properties of olfactory ensheathing cells that may contribute to neural repair and protection following spinal cord injury. Neurosci. Lett. 456, 137–142.

Kubasak, M.D., Jindrich, D.L., Zhong, H., Takeoka, A., McFarland, K.C., Munoz-Quiles, C., Roy, R.R., Edgerton, V.R., Ramon-Cueto, A., Phelps, P.E., 2008. OEG implantation and step training enhance hindlimb-stepping ability in adult spinal transected rats. Brain 131, 264–276.

Lakatos, A., Franklin, R.J., Barnett, S.C., 2000. Olfactory ensheathing cells and Schwann cells differ in their in vitro interactions with astrocytes. Glia 32, 214–225.

Li, Y., Carlstedt, T., Berthold, C.H., Raisman, G., 2004. Interaction of transplanted olfactory-ensheathing cells and host astrocytic processes provides a bridge for axons to regenerate across the dorsal root entry zone. Exp. Neurol. 188, 300–308.

Lipski, J., Zhang, X., Kruszewska, B., Kanjhan, R., 1994. Morphological study of long axonal projections of ventral medullary inspiratory neurons in the rat. Brain Res. 640, 171–184.

Lopez-Vales, R., Fores, J., Navarro, X., Verdu, E., 2006. Olfactory ensheathing glia graft in combination with FK506 administration promote repair after spinal cord injury. Neurobiol. Dis. 24, 443–454.

Lopez-Vales, R., Fores, J., Navarro, X., Verdu, E., 2007. Chronic transplantation of olfactory ensheathing cells promotes partial recovery after complete spinal cord transection in the rat. Glia 55, 303–311.

Lu, J., Feron, F., Ho, S.M., Mackay-Sim, A., Waite, P.M., 2001. Transplantation of nasal olfactory tissue promotes partial recovery in paraplegic adult rats. Brain Res. 889, 344–357.

Mackay-Sim, A., Feron, F., Cochrane, J., Bassingthwaighte, L., Bayliss, C., Davies, W., Fronek, P., Gray, C., Kerr, G., Licina, P., Nowitzke, A., Perry, C., Silburn, P.A., Urquhart, S., Geraghty, T., 2008. Autologous olfactory ensheathing cell transplantation in human paraplegia: a 3 year clinical trial. Brain 131, 2376–2386.

Martini, R., Schachner, M., Brushart, T.M., 1994. The L2/HNK-1 carbohydrate is preferentially expressed by previously motor axon-associated Schwann cells in reinnervated peripheral nerves. J. Neurosci. 14, 7180–7191.

Newton, B.W., Maley, B.E., Hamill, R.W., 1986. Immunohistochemical demonstration of serotonin neurons in autonomic regions of the rat spinal cord. Brain Res. 376, 155–163.

Peyronnet, J., Roux, J.C., Geloen, A., Tang, L.Q., Pequignot, J.M., Lagercrantz, H., Dalmaz, Y., 2000. Prenatal hypoxia impairs the postnatal development of neural and functional chemoafferent pathway in rat. J. Physiol. 524 (Pt 2), 525–537.

Polentes, J., Stamegna, J.C., Nieto-Sampedro, M., Gauthier, P., 2004. Phrenic rehabilitation and diaphragm recovery after cervical injury and transplantation of olfactory ensheathing cells. Neurobiol. Dis. 16, 638–653.

Raisman, G., Li, Y., 2007. Repair of neural pathways by olfactory ensheathing cells. Nat. Rev. Neurosci. 8, 312–319.

Ramer, L.M., Au, E., Richter, M.W., Liu, J., Tetzlaff, W., Roskams, A.J., 2004. Peripheral olfactory ensheathing cells reduce scar and cavity formation and promote regeneration after spinal cord injury. J. Comp. Neurol. 473, 1–15.

Ramon-Cueto, A., Nieto-Sampedro, M., 1994. Regeneration into the spinal cord of transected dorsal root axons is promoted by ensheathing glia transplants. Exp. Neurol. 127, 232–244.

Ramon-Cueto, A., Plant, G.W., Avila, J., Bunge, M.B., 1998. Long-distance axonal regeneration in the transected adult rat spinal cord is promoted by olfactory ensheathing glia transplants. J. Neurosci. 18, 3803–3815.

Richter, M.W., Roskams, A.J., 2008. Olfactory ensheathing cell transplantation following spinal cord injury: hype or hope? Exp. Neurol. 209, 353–367.

Richter, M.W., Fletcher, P.A., Liu, J., Tetzlaff, W., Roskams, A.J., 2005. Lamina propria and olfactory bulb ensheathing cells exhibit differential integration and migration and promote differential axon sprouting in the lesioned spinal cord. J. Neurosci. 25, 10700–10711.

Saito, H., Nakao, Y., Takayama, S., Toyama, Y., Asou, H., 2005. Specific expression of an HNK-1 carbohydrate epitope and NCAM on femoral nerve Schwann cells in mice. Neurosci. Res. 53, 314–322.

Santos-Silva, A., Fairless, R., Frame, M.C., Montague, P., Smith, G.M., Toft, A., Riddell, J.S., Barnett, S.C., 2007. FGF/heparin differentially regulates Schwann cell and olfactory

ensheathing cell interactions with astrocytes: a role in astrocytosis. J. Neurosci. 27, 7154–7167.
Sasaki, M., Lankford, K.L., Zemedkun, M., Kocsis, J.D., 2004. Identified olfactory ensheathing cells transplanted into the transected dorsal funiculus bridge the lesion and form myelin. J. Neurosci. 24, 8485–8493.
Speck, D.F., 1988. Respiratory resetting induced by spinal cord stimulation in the cat. J. Appl. Physiol. 65, 1572–1578.
Takeoka, A., Kubasak, M.D., Zhong, H., Roy, R.R., Phelps, P.E., 2009. Serotonergic innervation of the caudal spinal stump in rats after complete spinal transection: effect of olfactory ensheathing glia. J. Comp. Neurol. 515, 664–676.
Tian, D.S., Dong, Q., Pan, D.J., He, Y., Yu, Z.Y., Xie, M.J., Wang, W., 2007. Attenuation of astrogliosis by suppressing of microglial proliferation with the cell cycle inhibitor olomoucine in rat spinal cord injury model. Brain Res. 1154, 206–214.